

DESIGN OF A PASSIVE AND PORTABLE DMFC OPERATING IN ALL ORIENTATIONS

N. Paust¹, S. Krumbholz², S. Munt¹, C. Müller¹, R. Zengerle¹, C. Ziegler¹, and P. Koltay¹

¹University of Freiburg - IMTEK, Georges-Koehler-Allee 106, 79110 Freiburg, Germany

²Fraunhofer IZM, Gustav-Meyer-Allee 25, 13355 Berlin, Germany

ABSTRACT

A microfluidic layout concept for passive and portable Direct Methanol fuel Cells (DMFCs) is presented. We proofed this concept by developing a DMFC that continuously runs for 40 hours in all orientations without the need for any active components such as pumps or valves. In contrast to our previous work [1], the system now is truly portable. In any orientation of the DMFC, a bubble driven self regulating supply mechanism safely removes carbon dioxide and transports at least 3.5 times more methanol to the anode than critically needed to sustain DMFC operation. On the cathode, diffusive oxygen supply and the transport of the reaction product water along a capillary gradient out of the DMFC ensures a stable performance. Compared to our previous work [1], the power output was increased by a factor of 2.5 and reached $p = 5.5 \text{ mW cm}^{-2}$. A stable power output for 40 hours of $p = 4 \text{ mW cm}^{-2}$ was achieved for the preferred vertical position with bubbles moving against buoyancy forces. In the most challenging horizontal position with the anode facing downwards, a power output of at least $p = 3.1 \text{ mW cm}^{-2}$ was reached for the same period of time.

INTRODUCTION

Passive concepts for fuel supply are very attractive for miniaturized Direct Methanol Fuel Cells (DMFCs) [2-4]. Passive in this context means that the DMFC operates fully autonomously without any support of any kind. The abandonment of ancillary pumps and valves makes the system small and compact, increasing the overall energy density. Thus, the passive DMFC is a promising candidate for power supply of small portable appliances. However, a stable long-term performance in all orientations of the fuel cell poses a significant challenge [5]. Methanol supply and the removal of the reaction product carbon dioxide (CO_2) on the anode, as well as oxygen supply and water removal on the cathode must be achieved in any orientation independent of gravity. In our passive DMFC, effects dominant on the micro-scale such as diffusion and capillary force induced transport are applied to account for this challenge.

DESIGN AND OPERATING PRINCIPLE

A schematic of the passive and portable DMFC is depicted in Fig. 1. In the present work, our previously presented passive fuel supply mechanism on the anode [1], propelled by capillary forces of deformed CO_2 bubbles in tapered channel structures, is embedded into a closed design concept. First, the main channel parameters for the anode flow field are determined by analytical calculations ensuring that the capillary pressure gradients are sufficiently large to transport bubbles along the channel even against buoyancy forces. Secondly, the liquid flow rates induced by the

bubbly CO_2 gas flow is studied by experiments or Computational Fluid Dynamics (CFD) simulations ensuring that a sufficient amount of methanol is supplied for DMFC operation. In a third step, the channel parameters of the cathode flowfield are determined by CFD-simulations considering diffusive oxygen transport. Subsequently, water formation and transport on the cathode have to be accounted for and the flowfield design is refined to achieve capillary transport of water out of the DMFC by a continuous capillary gradient, hence, the oxygen supply is never blocked.

An exploded view of the current version of our passive DMFC is depicted in Fig. 2. The anode flow field consists of six parallel channels fabricated by micro milling in transparent COC. Each channel has an inlet height of $h_{in} = 0.2\text{mm}$, is $w = 1.2\text{mm}$ wide, has an opening angle of $\alpha = 4^\circ$ and is $l = 14.3\text{mm}$ long. The channels are coated with a hydrophilic polymer by dip coating with DMAAm-MaBP [6] which results in contact angles at the walls of $\theta = 10^\circ$. At the end of the channels, the CO_2 gas phase is separated from the liquid by a hydrophobic membrane (Fig. 1 (2)) (Whatman PTFE TE36) that holds back the liquid by capillary forces and a bubble fence (Fig. 1 (3)) that allows for the liquid phase to pass but holds back the gas, again, by capillary forces. The bubble fence consists of 20 hydrophilic coated COC poles with a diameter of $d = 300\mu\text{m}$ arranged with gaps of $D = 200\mu\text{m}$. The bubbles moving along the tapered channels pump the methanol solution through the bubble fence and the tubing into the reservoir and leave the system through the hydrophobic membrane.

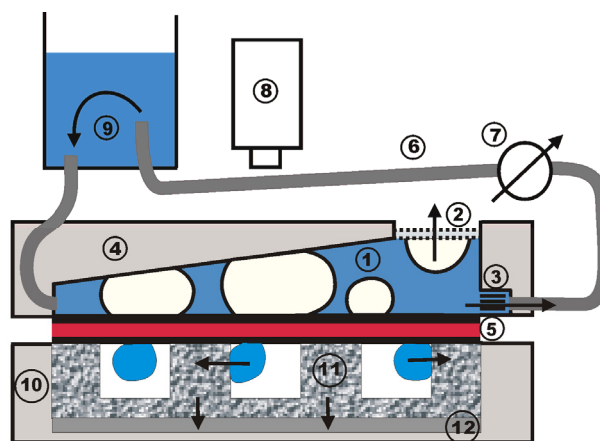


Figure 1: Schematic of the passive DMFC. 1) Tapered channel; 2) Hydrophobic membrane; 3) Bubble fence; 4) Transparent anode flow field; 5) GDL and MEA; 6) Tubing; 7) Flow sensor; 8) Camera; 9) Reservoir; 10) Cathode mount; 11) Cathode flow field; 12) Non woven material for capillary water transport.

Simultaneously, the bubble movement sucks liquid from the reservoir into the narrow channel end. Thus, a net circulation of methanol is induced that supplies the DMFC with fuel as described in detail in [1].

The channels feature an active area of $A = 2.6 \text{ cm}^2$. Since the flowfield consists of non-conductive COC, a current collector is added (Fig. 2 (4)) that was manufactured by laser cutting of stainless steel and electroplated with a $5 \mu\text{m}$ gold layer. The current collector is separated from the Membrane Electrode Assembly (MEA) (catalyst coated @Nafion N115; Anode: 3 mg cm^{-2} PtRu; Cathode: 1.3 mg cm^{-2} Pt manufactured by balticFuelCells) by a gas diffusion layer GDL (SGL, @SIGRACET GDL31-BA) that was made hydrophilic by plasma activation in order to increase the bubble mobility in the flow field channels. The anode is sealed by a vacuum casted PDMS layer.

At the cathode side, the GDL (SGL, @SIGRACET S10CC) is hydrophobic containing 10% weight of PTFE in order to keep the GDL free from liquid water which would hinder oxygen supply. The cathode flow field consists of porous carbon (SGL, PGP) (Fig. 2 (9)) that was also made hydrophilic by plasma activation. Channels in cross direction to the methanol channels on the anode are milled into the carbon. The cross section of these channels is $h_1 \times w_1 = 1 \text{ mm} \times 1 \text{ mm}$. In order to enhance diffusion of oxygen, on the back side of the porous carbon channels are milled with a cross section of $h_2 \times w_2 = 2 \text{ mm} \times 1.5 \text{ mm}$ in cross direction to the channels on the MEA facing side. A droplet emerging from or forming on the hydrophobic GDL moves into the bulk material of the porous carbon as soon as it touches the channel walls. The water is further transported out of the DMFC by non woven material where it finally evaporates. Thus, the channels are never blocked and diffusive oxygen supply is guaranteed in all orientations of the operating DMFC.

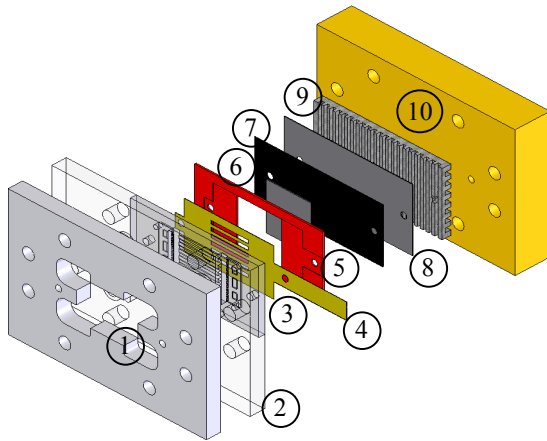


Figure 2: Exploded view on the passive DMFC.

1) Aluminum support plate 2) Transparent end plate;
3) Anode flow field; 4) Current collector; 5) Vacuum casted PDMS sealing; 6) Anode GDL 7) MEA; 8) Cathode GDL; 9) Cathode flow field; 10) Conductive end plate.

RESULTS

The passive fuel delivery on the anode was measured with a flow sensor and is evaluated by the pump efficiency p_{eff} , defined as the ratio of the measured volumetric liquid flow rate to the bubbly CO_2 gas flow rate. During passive operation, it is assumed that the liquid is saturated with CO_2 , thus all CO_2 is generated in the gaseous phase and the volumetric gas flow rate density Φ_{gas} per unit area of the MEA can be calculated by the current density i , the molar weight M_{CO_2} and the density ρ_{CO_2} as follows:

$$\Phi_{gas} = \frac{M_{\text{CO}_2} i}{\rho_{\text{CO}_2} 6F} \quad (1)$$

where F is the Faraday constant.

Fig. 3 shows the liquid flow rate density induced by moving gas bubbles and the electrical current for two load cycles plotted against time. The load cycle was performed in a horizontal position with galvanostatic steps ($\Delta t = 10 \text{ s}$; $i_{step} = 7.7 \text{ mA cm}^{-2}$). Comparison with pressure signals showed that each peak of the flow rate density is actually caused by single bubbles that move through the channel and pump methanol. The floating average with a time span of 10s shows peaks and minima at the same time as the electrical load. At the first peak, $p_{eff} = 22\%$ was determined and for the second peak $p_{eff} = 20\%$. Considering the average current density and the average flow rate density over the two complete cycles, the pump efficiency yields $p_{eff} = 19\%$. The liquid flow rate density closely follows the electrical load and the methanol supply is regulated by the passive anode flow field with a response time of less than 10 seconds whereas a response time of several minutes would be sufficient due to the storage of methanol in the channel and the GDL.

In Fig. 4, the average pump efficiency of the anode of the DMFC is plotted against the current density for different DMFC orientations. Each data point was acquired by averaging the flow rates over 10 minutes and repeating the measurements 3 times on different days.

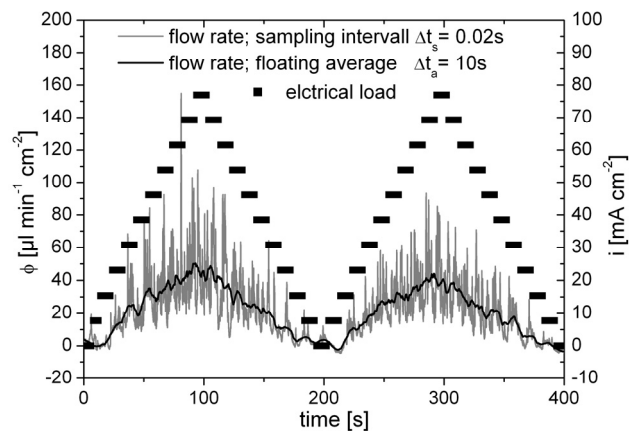


Figure 3: Current density and flow rate density plotted against time for two galvanostatic load cycles; $T = 23^\circ\text{C}$.

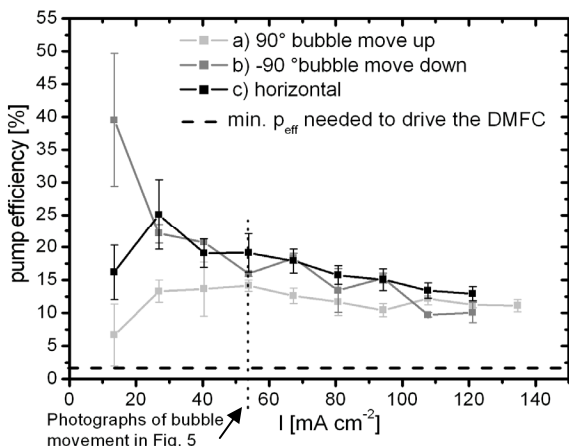


Figure 4: Pump efficiency p_{eff} plotted against the electrical load for different cell orientations; $T = 50^{\circ}\text{C}$.

The smallest p_{eff} was measured at a current density of $i = 13.5 \text{ mA cm}^{-2}$ in a vertical position with the bubbles moving upwards driven by buoyancy forces (Fig. 4 light grey line). The reason for the small p_{eff} is the dominating non-blocking pumping mode in this configuration which can be understood as follows: As depicted in Fig. 5 (a), driven by buoyancy forces, comparably small bubbles that do not fill the cross section of the tapered channel move along the channel from the smaller to the larger cross section. As discussed in our previous work [5], in the non-blocking pumping mode, the major part of the liquid displaced by moving bubbles circulates directly around the bubbles and only a minor part contributes to the pump mechanism. As the bubble generation frequency increases with increasing current densities more liquid is dragged in pump direction by the numerous bubbles moving in the non blocking mode and p_{eff} first increases with an increasing electrical load. As the load increases further p_{eff} remains roughly constant.

The largest p_{eff} occurs at low current densities with the capillary movement of bubbles against buoyancy forces (Fig. 4 dark grey line and Fig. 5 (b)). In this orientation, driven by buoyancy forces, small bubbles move in the opposite direction of the overall pump direction. In the narrower part of the channel these bubbles are caught either by the upper and lower channel wall or by a bubble that has been formed previously. Bubbles grow from the narrow part of the channel towards the increasing cross section. When these bubbles exceed a certain size, the capillary forces of the bubbles that are deformed by the tapered channel walls overcome the buoyancy forces and the bubbles move in the blocking pumping mode towards the larger cross section of the channel. Since these large gas bubbles first form at the inlet and then move through the complete channel, a comparably large amount of liquid is transported by these bubbles. With increasing current densities, blocking bubbles also form in the middle of the channel, thus, less liquid is transported by these bubbles and p_{eff} decreases with an increasing electrical load.

In the horizontal orientation (Fig. 4 black line and Fig. 5 (c)), small bubbles remain fixed due to contact line pinning [1] and large bubbles move in pump direction in the

blocking mode. The size of the liquid segments enclosed by moving bubbles in the blocking mode decreases with increasing current densities, thus, a slight decline of p_{eff} can be observed with an increasing electrical load.

In all orientations, the measured pump efficiency was between $p_{eff} = 7\%$ and $p_{eff} = 40\%$. The minimum pump efficiency for a 2 molar methanol solution as considered in this work is $p_{eff,min} = 2\%$, hence, 3.5 up to 20 times more fuel than critically needed to operate the DMFC was supplied to the anode which proves the mechanism to be suitable for fuel supply in portable DMFCs.

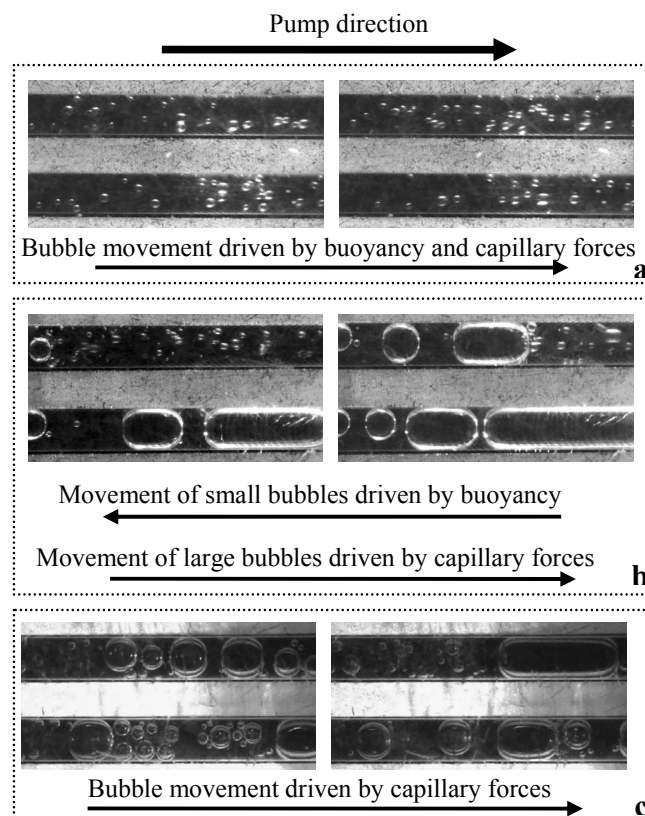


Figure 5: Top views on moving bubbles in two of the six anode channels; Electrical load: $I = 53.8 \text{ mA cm}^{-2}$. The difference in time between the left and the right pictures is $\Delta t = 5.7\text{s}$.

a) Vertical orientation with the bubbles moving upwards; b) Vertical orientation with the bubbles moving downwards against buoyancy forces; c) Horizontal orientation.

In Fig. 6 the polarization curve of the passive DMFC operating at ambient temperature and pressure is depicted. For each plotted current density, measurements were performed every 10s for galvanostatic intervals of one hour. The complete measurement lasted ten hours. The maximum power density was reached at $i = 35 \text{ mA cm}^{-2}$ with a power output of $p = 5.5 \text{ mW cm}^{-2}$. Comparably low fluctuations (less than 12 mV) of the voltage were measured for current densities between $i = 15 \text{ mA cm}^{-2}$ and $i = 35 \text{ mA cm}^{-2}$. This operation range shows a stable performance where a sufficient amount of fuel is transported to both, the anode and the cathode of the DMFC. The long term performance of the passive DMFC for a current density of $i = 17.3 \text{ mA cm}^{-2}$ is depicted in Fig. 7.

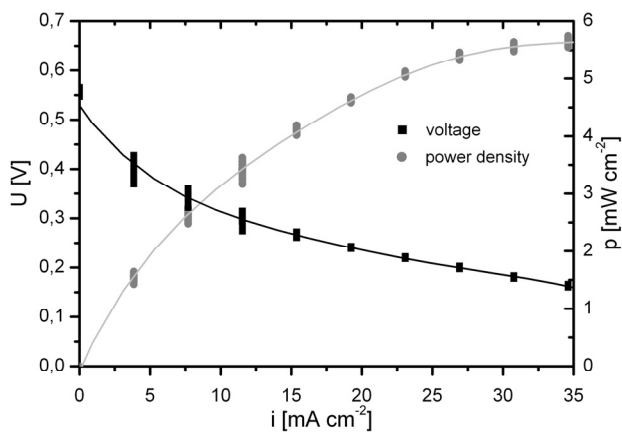


Figure 6: Polarization curve of the passively operating DMFC with galvanostatic intervals of one hour; $T=23^{\circ}\text{C}$.

First, as a control experiment, measurements were performed for the vertical orientation using a cathode flowfield without capillary water removal. The power density declined rapidly from $p = 4.3 \text{ mW cm}^{-2}$ to less than 2 mW cm^{-2} within the first 5 hours of operation (Fig. 7 light grey line). The reason for the comparably bad performance is that water accumulates in the channels (see Fig. 8 (a)) and blocks the oxygen supply to the active area of the cathode. In contrast, when using the new cathode flowfield water is transported through the porous carbon and the non woven material out of the DMFC where the water finally evaporates. This feature allows for a stable long-term performance, thus, in the same vertical orientation, a continuous operation of more than 40 hours was observed with a power decline of less than 12 %.

Finally, the DMFC was tested in the most challenging position with the anode facing downwards. In this position the buoyancy of the CO_2 gas pushes the bubbles against the active area of the anode and on the cathode gravity does the same to the water. The power output declines from initially $p = 4.5 \text{ mW cm}^{-2}$ to $p = 3.1 \text{ mW cm}^{-2}$. We assume that this decline is due to the formation of a water film between the catalyst layer and GDL. When taking apart the DMFC after this measurement, the catalyst on the cathode showed comparably large wet spots. Passive management of fluids between the GDL and MEA has not been addressed in this study but might improve the performance of the DMFC.

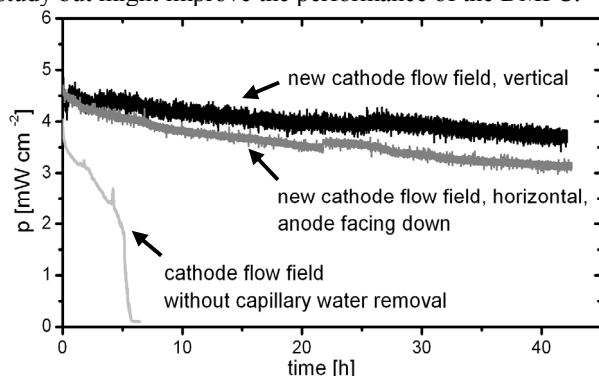


Figure 7: Long term performance of the passive DMFC for different orientations and different cathode flow fields; $i = 17.3 \text{ mA cm}^{-2}$; $T = 23^{\circ}\text{C}$.

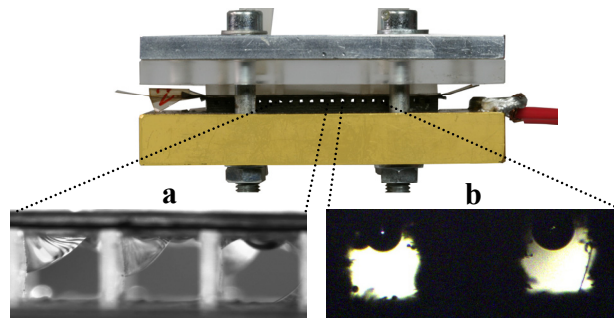


Figure 8: Front view photograph of the passive DMFC with enlarged cathode channels. a) Water accumulates in a conventional cathode flow field; b) The porous carbon flow field removes water as soon as droplets touch the side walls of the channels. Small droplets remain.

CONCLUSIONS

The presented layout concept enables the design of a passive, compact, and portable DMFC that operates in all orientations. On the anode between 3.5 and 20 times more methanol than critically needed to supply the DMFC is transported by the supply mechanism driven by capillary movement of CO_2 bubbles. The flow rates induced by the moving bubbles closely follow the electrical load, thus, the mechanism can be considered as self regulating. On the cathode, oxygen is supplied by diffusion and abundant water is transported out of the DMFC along a continuous capillary gradient. With these features, the DMFC exhibited a stable operation for more than 40 hours in all orientations. This is a major step towards the usage of passive DMFCs in portable systems. To further improve the performance of the DMFC, the fluid management should be extended to the area between the GDL and the MEA.

ACKNOWLEDGEMENTS

This work was supported by the German Ministry of Science and Education within Project 03SF0311B.

REFERENCES

- [1] N. Paust, et. al., "Fully Passive Degassing and Fuel Supply in Direct Methanol Fuel Cells," in Proc. of the 21st IEEE MEMS, Tucson, USA 2008, pp. 34-37
- [2] B. Bae et. al., "Performance evaluation of passive DMFC single cells," in *J. Power Sources*, vol. 158, no. 2, pp. 1256-1261, Aug.2006
- [3] T. Shimizu et. al., "Design and fabrication of pumpless small direct methanol fuel cells for portable applications," in *J. Power Sources*, vol. 137, no. 2, pp. 277-283, Oct.2004
- [4] Y. H. Chan, et. al., "A small mono-polar direct methanol fuel cell stack with passive operation," in *J. Power Sources*, vol. 176, pp. 183-190, Dec.2007
- [5] R. Chen, et. al., "Effect of cell orientation on the performance of a passive direct methanol fuel cell," in *J. Power Sources*, vol. 157, pp. 351-357, Oct.2005
- [6] R. Toomey, et. al., "Swelling Behavior of Thin, Surface-Attached Polymer Networks," in *Macromolecules*, vol. 37, pp. 882-887, 2004